

## COMPUTING RADIATIVE HEAT TRANSFER OCCURRING IN A ZONE FIRE MODEL

Glenn P. Forney

National Institute of Standards and Technology,  
Gaithersburg, MD 20899, U.S.A.

(Received August 5, 1993, Accepted August 3, 1994)

### ABSTRACT

Radiation, convection and conduction are the three mechanisms which a zone fire model must consider when calculating the heat transfer between fires, wall surfaces and room gases. Radiation dominates the other two modes of heat transfer in rooms where there are fires or hot smoke layers. The computational requirements of a radiation model can also easily dominate the work required to calculate other physical sub-models in a zone fire model.

This paper presents algorithms for efficiently computing the radiative heat exchange between four wall surfaces, several fires and two interior gases. A two-wall and a ten-wall radiation model are also discussed. The structure of this radiation model is exploited to show that only a few configuration factors need to be calculated directly (two rather than 16 for the four-wall model and eight rather than 100 for the ten-wall model) and matrices needed to solve for the net radiative flux striking each surface are shown, after the appropriate transformation is taken, to be diagonally dominant. Iterative methods may then be used to solve the linear equations more efficiently than direct methods such as Gaussian elimination.

### INTRODUCTION

Radiation is an important heat transfer mode to represent in a zone fire model due to the high temperatures attained in rooms with fires or hot smoke layers. It can easily dominate convective and conductive heat transfer. A radiative heat transfer calculation can also easily dominate the computation in any fire model. This is because radiation exchange is a global phenomena. Each portion of an enclosure interacts radiatively with every other portion that it 'sees'. It is therefore important to design radiation exchange algorithms that are *efficient* as well as *accurate*.

Most zone fire models use two wall segments to model radiation exchange. Harvard V [1], FIRST [2], BRI [3, 4] and FAST [5] are some examples. FAST/FFM [6] on the other hand uses many surface segments in order to model the radiative interaction between wall surfaces and furniture elements. Harvard V, FIRST, BRI and FAST model the two wall segments as an extended floor and ceiling. The extended ceiling consists of the ceiling plus the four upper walls. The upper wall is the portion of a wall above the layer interface. Likewise, the lower wall is below the interface. The extended floor consists of the floor plus the four lower walls. The purpose of the work described in this paper then is to enhance two wall radiation exchange algorithms by considering more wall segments. In particular for the four-wall case, this allows the ceiling, the upper wall segment, the lower wall seg-

ment and the floor to transfer radiant heat independently.

This paper describes three related algorithms for computing radiative heat transfer between the bounding surfaces of a compartment containing upper and lower layer gases and point source fires. The first algorithm uses two wall segments, the second uses four wall segments and the third uses ten wall segments. These algorithms each use the net radiation equation as described in Siegel and Howell [7, Chapter 17] which is based on Hottel's work in [8]. An enclosure is modeled with N wall segments (for our case N will be 2, 4 or 10) and an interior gas. A two layer zone fire model, however, requires treatment of an enclosure with two uniform gases (the upper and lower layer). Hottel and Cohen [9] developed a method to handle this case by dividing an enclosure into a number of wall and gas volume elements. Treatment of the fire and the interaction of the fire and gas layers with the walls is based upon the work of Yamada and Cooper [10, 11] on N-wall radiation exchange models. They model the fire as a point source of heat radiating uniformly in all directions and use the Lambert-Beer law to model the interaction between heat emitting objects (fires, walls or gas layers for example) and gas layers.

The two, four and ten wall algorithms are implemented as FORTRAN 77 subroutines named RAD2, RAD4 and RAD10. The routines, RAD2 and RAD10, take advantage of the modular structure of RAD4 by using a number of its routines. It should be pointed out that

the computational requirements of a general N-wall radiation model are too great for now to justify incorporating it into a zone fire model. By implementing the net radiation equation for particular N (two, four or ten walls), significant algorithmic speed increases were achieved by exploiting the structure of the simpler problems.

## THE PROBLEM

### N Wall Segment Radiation Exchange

The N-wall radiation model described here considers radiative heat transfer between wall segments, point-source fires and two gas layers. An enclosure or room is partitioned into N wall segments where each wall segment emits, reflects and absorbs radiant energy. The interior of the enclosure is partitioned into two volume elements; an upper and a lower layer. The problem then is to determine the net radiation flux emitted by each wall segment and the energy absorbed by each layer given the temperature and emittance of each wall segment and the temperature and absorptance of the two gas layers.

These calculations can be performed in conjunction with a zone fire model such as CFAST[12]. Typically, the solution (wall temperatures, gas layer temperatures *etc*) is known at a given time  $t$ . The solution is then advanced to a new time,  $t + \Delta t$ . The calculated radiation fluxes along with convective fluxes are used as a boundary condition for an associated heat conduction problem in order to calculate wall temperatures. Gas layer energy absorption due to radiation contributes to the energy source terms of the associated zone fire modeling differential equations. The time step,  $\Delta t$ , must be chosen sufficiently small so that changes in wall temperatures are small over the duration of the time step.

**Modeling Assumptions** The following assumptions are made in order to simplify the radiation heat exchange model and to make its calculation tractable.

**iso-thermal** Each gas layer and each wall segment is assumed to be at a uniform temperature. This assumption breaks down where wall segments meet.

**equilibrium** The wall segments and gas layers are assumed to be in a quasi-steady state. The wall and gas layer temperatures are assumed to change slowly over the duration of the time step of the associated differential equation.

**fire source** The fire is assumed to radiate uni-

formly in all directions from a single point giving off a fraction,  $\chi$ , of the total energy release rate to thermal radiation.

**radiators** The radiation emitted from a wall surface, a gas and a fire is assumed to be diffuse and gray. In other words, the radiant fluxes emitted by these objects are independent of the direction and the wavelength. They can depend on temperature, however. Since both the emittances and the temperatures of wall segments are inputs to the radiation algorithms, it is assumed that the emittances are consistent with the corresponding wall temperatures. Diffusivity implies that  $\epsilon_\lambda = \alpha_\lambda$  for each wavelength  $\lambda$  while the gray gas/surface assumption implies that  $\epsilon_\lambda$  is constant for all wavelengths. These assumptions allow us to infer that the emittance,  $\epsilon$  and absorptance,  $\alpha$  are related *via*  $\epsilon = \alpha$ . A discussion of this assumption can be found in [13, p. 589–590].

**opacity** The wall surfaces are assumed to be opaque. When radiation encounters a surface it is either reflected or absorbed. It is not transmitted through the surface. Equation (1), found below, would have to be modified to account for the loss (or gain) of energy through semi-transparent surfaces.

**geometry** Rooms or compartments are assumed to be rectangular boxes. Each wall is either perpendicular or parallel to every other wall. Radiation transfer through vent openings, doors, *etc* is neglected.

**The Net Radiation Equations** Net radiation refers to the difference between outgoing and incoming radiation at a wall surface. As illustrated in Figure 1, incoming radiation consists of gray-body surface radiation emitted from all other surfaces, radiating point-source fires and emission from the two gas layers. Outgoing radiation consists of gray-body surface radiation and incoming radiation that is in turn reflected. Integrating the net radiation equation in Segel and Howell[7, Chapter 17] over all wavelengths, we obtain an equation for the net radiation at each wall surface  $k$  given by

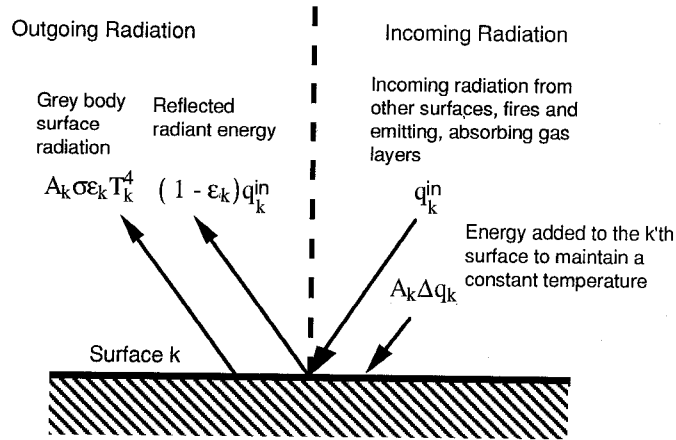


FIGURE 1: Input and Output Energy Distribution at the k'th Wall Surface

$$\frac{\Delta q''_k}{\epsilon_k} - \sum_{j=1}^N \frac{1 - \epsilon_j}{\epsilon_j} \Delta q''_j F_{k-j} \tau_{j-k} = \sigma T_k^4 - \sum_{j=1}^N \sigma T_j^4 F_{k-j} \tau_{j-k} - \frac{c_k}{A_k} \quad (1)$$

where  $\Delta q''_k$  is the unknown radiative flux and  $c_k/A_k$ , accounts for radiative flux striking the k'th wall surface due to point source fires and gas layers and is given by

$$\frac{c_k}{A_k} = \sum_{f=1}^{N_{fire}} q''_{f-k} + \sum_{j=1}^N (q''_{j-k}^{L,gas} + q''_{j-k}^{U,gas}) \quad (2)$$

Other terms are defined in the nomenclature. Wall openings (vents, doors, etc) can be modeled by replacing  $T_j$  in equation (1) with  $\hat{T}$  where

$$\hat{T}^4 = T_j^4 - \frac{A_v}{A_j} (T_j^4 - T_{amb}^4),$$

$A_v$  is the vent area and  $T_{amb}$  is the ambient temperature. Figure 2 presents a surface plot showing the effect of this equation. It plots the absolute temperature difference,  $(T - \hat{T})$ , versus relative vent area,  $A_v/A_j$ , and temperature,  $T$ . Note that over this broad range of temperatures and vent area fractions that the absolute change

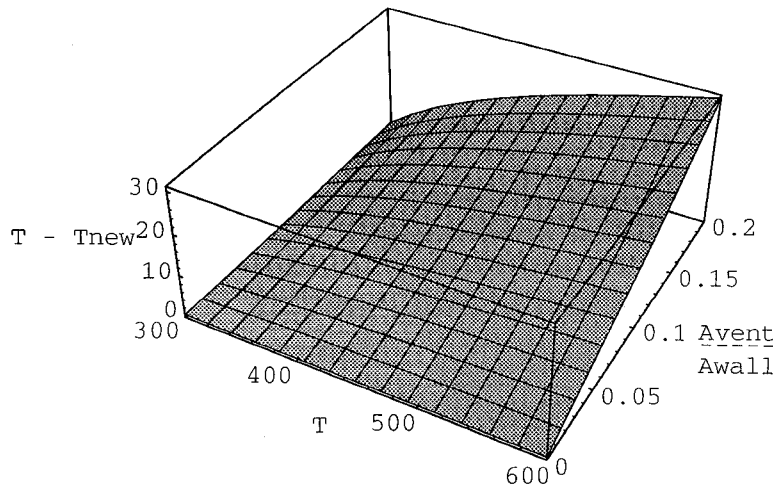


FIGURE 2: Surface plot of temperature difference (original temperature and equivalent temperature accounting for vents and doors) as a function of fractional vent area and temperature showing the effect of vent openings on computing radiation heat transfer.

in  $T$  required to account for vent openings is small. For large temperatures  $T$  or large vent fractions  $A_v/A_j$  then vent openings need to be taken into account.

Subsequent sections discuss the computation of terms in (1) and (2).

**Heat Flux Striking a Wall Segment** In general, every possible path between two wall segments should be considered in order to compute the total radiant heat transfer between these segments. This is not practical in a zone fire model due to the excessive computational costs. The approach taken here is to model this heat transfer using just one path. For a typical path there are four cases to consider. A path from wall segment  $j$  to  $k$  can start in either the upper or lower layer and finish in either the upper or lower layer. A fraction,  $\alpha = 1 - \tau$ , of the energy encountering a layer is absorbed. The rest,  $\tau$ , passes through unimpeded. Table 1 gives formulas for the heat flux striking the  $k$ 'th wall segment due to point source fires and heat emitting gas layers.

**Heat Flux Striking a Wall Segment Due to a Point Source Fire** If the gas layers are transparent then the flux striking the  $k$ 'th surface due to the  $f$ 'th fire is

$$q''_{f-k}{}^{fire} = \frac{\chi q_{total}^{fire} \omega_{f-k}}{4\pi A_k}$$

where the total energy release rate of the fire is  $q_{total}^{fire}$ ,  $\chi$  is the fraction of this energy that contributes to radiation and  $\omega_{f-k}/(4\pi A_k)$  is the fraction of the radiant energy leaving the  $f$ 'th fire that is intercepted by the  $k$ 'th wall segment, *ie* a configuration factor. On the other hand, if the gas layers are not transparent then there are four cases to consider. The fire can be in the upper or lower layer and the surface can be in the upper or lower layer. Figure 3 shows how radiation from a fire is absorbed by each layer when the fire is in the lower layer and the surface  $k$  is in the upper layer. The other three cases are handled similarly. These four cases are summarized in the first column of Table 1. This column give formulas

Table 1: Radiative Heat Flux Striking the  $k$ 'th Rectangular Wall Segment

Path	Fire	Gas Layer	
	$q''_{f-k}{}^{fire}$	$q''_{j-k}{}^{L,gas}$	$q''_{j-k}{}^{U,gas}$
in upper	$\tau_{f-k}^U \frac{\chi q_{total}^{fire} \omega_{f-k}}{4\pi A_k}$	0	$F_{k-j} \sigma \alpha_{j-k}^U T_U^4$
from upper to lower	$\tau_{f-k}^U \tau_{f-k}^L \frac{\chi q_{total}^{fire} \omega_{f-k}}{4\pi A_k}$	$F_{k-j} \sigma \alpha_{j-k}^L T_L^4$	$F_{k-j} \sigma \alpha_{j-k}^U T_U^4 \tau_{j-k}^L$
from lower to upper	$\tau_{f-k}^L \tau_{f-k}^U \frac{\chi q_{total}^{fire} \omega_{f-k}}{4\pi A_k}$	$F_{k-j} \sigma \alpha_{j-k}^L T_L^4 \tau_{j-k}^L$	$F_{k-j} \sigma \alpha_{j-k}^U T_U^4$
in lower	$\tau_{f-k}^L \frac{\chi q_{total}^{fire} \omega_{f-k}}{4\pi A_k}$	$F_{k-j} \sigma \alpha_{j-k}^L T_L^4$	0

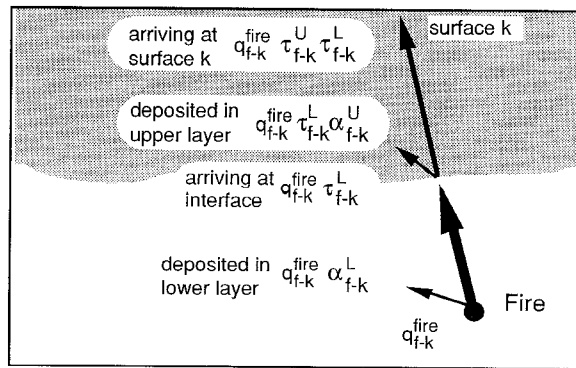


FIGURE 3: Schematic illustrating energy deposited into the lower layer,  $q''_{f-k}{}^{fire} \alpha_{f-k}^L$ , deposited into the upper layer,  $q''_{f-k}{}^{fire} \alpha_{f-k}^U \tau_{f-k}^L$ , and arriving at the  $k$ 'th wall surface,  $q''_{f-k}{}^{fire} \tau_{f-k}^L \tau_{f-k}^U$  due to the  $f$ 'th fire.

for the flux striking a surface k due to a point source fire.

**Heat Flux Striking a Wall Segment Due to an Emitting Gas Layer** The energy emitted by the i'th layer (i=upper, or i=lower) along the j-k'th path is

$$q''_{j-k}{}^{i, gas} = \alpha_{j-k}^i \sigma T_i^4$$

where  $\alpha_{j-k}^i = 1 - \tau_{j-k}^i$ . The emittance of the gas in this equation is the same as the absorptance due to the gray gas assumption. Again four cases must be considered to calculate the flux striking a wall segment. The last two columns of Table 1 gives formulas for radiation striking the k'th wall segment due to lower/upper gas layer heat emissions for each possible path.

**Gas Absorbance** The energy absorbed by the gas layers may be due to radiating wall segments, emission from other gas layers and radiation from fires. Tables 2 and 3 summarize the formulas used to compute gas layer energy gain/loss due to these phenomena. Again, there are four cases to consider, since an arbitrary path may start in either the lower or the upper layer and end in the lower or upper layer. Figure 4 illustrates the heat

absorbed by the gas layers due to surface rectangle emission where the "from" wall segment is in the upper layer and the "to" wall segment is in the lower layer. The other three cases are handled similarly.

**Configuration Factor Properties** A configuration factor,  $F_{j-k}$ , is the fraction of radiant energy leaving a surface j that is intercepted by a surface k. The following symmetry and additive properties (see [7, Chapter 7]) are used later to reduce the number of computations in the four-wall and ten-wall model

$$A_j F_{j-k} = A_k F_{k-j} \quad (3)$$

$$F_{i-j \oplus k} = F_{i-j} + F_{i-k} \quad (4)$$

$$A_{i \oplus j} F_{i \oplus j - k} = A_i F_{i-k} + A_j F_{j-k} \quad (5)$$

$$\sum_{k=1}^N F_{j-k} = 1, \quad j = 1, \dots, N \quad (6)$$

where  $i \oplus j$  denotes the union of two wall surfaces i and j. If four wall segments are configured as illustrated in Figure 5 then it can be shown that

$$A_1 F_{1-4} = A_2 F_{2-3} \quad (7)$$

Table 2: Radiant Heat Absorbed by the Upper Layer

Path through the Gas	Due to Heat Emitting Wall Surface $q_{j-k}^{out} = A_j F_{j-k} (\sigma T_j^4 - \frac{1-\epsilon_j}{\epsilon_j} \Delta q''_j)$	Due to Gas Layer Emission $q''_{j-k}{}^{i, gas} = \alpha_{j-k}^i \sigma T_i^4$ $q_{j-k}{}^{i, gas} = q''_{j-k}{}^{i, gas} A_j F_{j-k}$	Due to Point Source Fire $q''_{f-k}{}^{fire} = \frac{\chi q_{total}^{fire} \omega_{f-k}}{4\pi A_k}$
from the upper to either the lower or upper layer	$q_{j-k}^{out} \alpha_{j-k}^U$	$-q_{j-k}^{U, gas}$	$q''_{f-k}{}^{fire} \alpha_{f-k}^U$
from the lower to the upper layer	$q_{j-k}^{out} \tau_{j-k}^L \alpha_{j-k}^U$	$q_{j-k}^{L, gas} \alpha_{j-k}^U - q_{j-k}^{U, gas}$	$q''_{f-k}{}^{fire} \alpha_{f-k}^U \tau_{f-k}^L$
from the lower to the lower layer	0	0	0

Table 3: Radiant Heat Absorbed by the Lower Layer

Path through the Gas	Due to Heat Emitting Wall Surface $q_{j-k}^{out} = A_j F_{j-k} \left( \sigma T_j^4 - \frac{1-\epsilon_j}{\epsilon_j} \Delta q''_j \right)$	Due to Gas Layer Emission $q_{j-k}^{i,gas} = \alpha_{j-k}^i \sigma T_i^4$ $q_{j-k}^{i,gas} = q_{j-k}^{i,gas} A_j F_{j-k}$	Due to Point Source Fire $q''_{f-k}^{fire} = \frac{\chi q_{total}^{fire} \omega_{f-k}}{4\pi A_k}$
from the lower to either the lower or upper layer	$q_{j-k}^{out} \alpha_{j-k}^L$	$-q_{j-k}^{L,gas}$	$q''_{f-k}^{fire} \alpha_{f-k}^L$
from the upper to the lower layer	$q_{j-k}^{out} \tau_{j-k}^U \alpha_{j-k}^L$	$q_{j-k}^{U,gas} \alpha_{j-k}^L - q_{j-k}^{L,gas}$	$q''_{j-k}^{fire} \alpha_{f-k}^L \tau_{j-k}^U$
from the upper to the upper layer	0	0	0

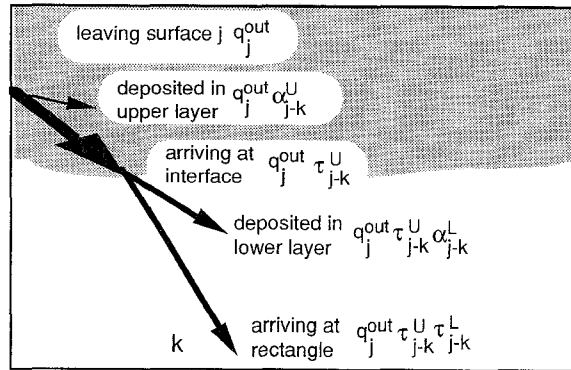


FIGURE 4: Schematic illustrating energy deposited into the upper layer,  $q_j^{out} \alpha_{j-k}^U$ , deposited in lower layer,  $q_j^{out} \tau_{j-k}^U \alpha_{j-k}^L$ , and arriving at the  $k$ 'th wall surface,  $q_j^{out} \tau_{j-k}^U \tau_{j-k}^L$  due to the  $j$ 'th wall surface.

$$A_1 F_{1-4} = A_2 F_{2-3}$$

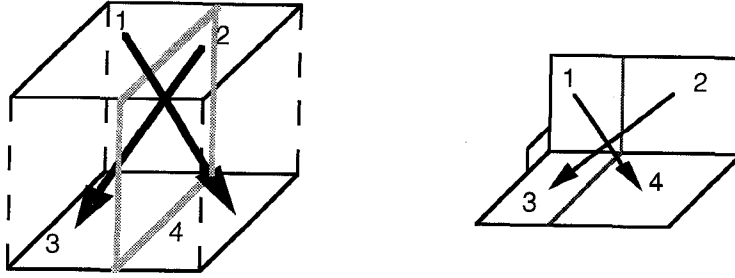


FIGURE 5: Configuration factor symmetries used to reduce number of direct configuration factor calculations.

The configuration factor between two rectangles with a common edge of length  $l$  lying on perpendicular planes can be found in [7, p. 825] to be

$$\begin{aligned} \phi_{perp}(h, l, w) = & \frac{1}{\pi W} \left\{ W \tan^{-1} \frac{1}{W} + H \tan^{-1} \frac{1}{H} - \right. \\ & \left. \sqrt{H^2 + W^2} \tan^{-1} \frac{1}{\sqrt{H^2 + W^2}} + \right. \\ & \left. \frac{1}{4} \log \left\{ \frac{(1 + W^2)(1 + H^2)}{1 + H^2 + W^2} \left[ \frac{W^2(1 + H^2 + W^2)}{(1 + W^2)(H^2 + W^2)} \right]^{W^2} \right. \right. \\ & \left. \left. \times \left[ \frac{H^2(1 + H^2 + W^2)}{(1 + W^2)(H^2 + W^2)} \right]^{H^2} \right\} \right\} \end{aligned} \quad (8)$$

where  $H = h/l$  and  $W = w/l$  and the two rectangles have dimensions  $l \times h$  and  $l \times w$ . Similarly, the configuration factor between two rectangles lying on parallel planes, a distance  $c$  apart can be found in [7, p. 824] to be

$$\begin{aligned} \phi_{par}(a, b, c) = & \frac{2}{\pi XY} \left\{ \log \sqrt{\frac{(1 + X^2)(1 + Y^2)}{1 + X^2 + Y^2}} + \right. \\ & X \sqrt{1 + Y^2} \tan^{-1} \frac{X}{1 + Y^2} + \\ & Y \sqrt{1 + X^2} \tan^{-1} \frac{Y}{1 + X^2} - \\ & \left. X \tan^{-1} X - Y \tan^{-1} Y \right\} \end{aligned} \quad (10)$$

where  $X = a/c$  and  $Y = b/c$  and the two rectangles each have dimension  $a \times b$ .

For a room with  $N$  wall segments,  $N \times N = N^2$  configuration factors must be calculated. Equations (8) and

(10) are expensive to compute due to the complicated expressions involving log and  $\tan^{-1}$  functions. This portion of the work is reduced in RAD4 by noting that only 2 configuration factor calculations involving equation (8) are required rather than  $4 \times 4 = 16$ . The other 14 configuration factors are obtained using algebraic relationships. For the RAD10 case only eight configuration factor calculations need be calculated using equations (8) and (10). Again, the other 92 can be obtained using algebraic formulas. These formulas are detailed in [14].

**Solid Angles** The fraction of a radiating point-source fire striking a wall surface is determined using solid angles. For a wall surface with sides of length  $x$  and  $y$  that lies in a plane a distance  $r$  from the fire the solid angle is

$$\begin{aligned} \omega(x, y) = & \frac{1}{4\pi} \left\{ \sin^{-1} \left( A \frac{y}{\sqrt{y^2 + r^2}} \right) + \right. \\ & \left. \sin^{-1} \left( A \frac{x}{\sqrt{x^2 + r^2}} \right) - \frac{\pi}{2} \right\} \end{aligned} \quad (11)$$

where

$$A = \sqrt{1 + \frac{r^2}{x^2 + y^2}}$$

The solid angle  $\omega(x, y)$  is symmetric in  $x$  and  $y$ . Solid angles are also additive, so that the solid angle of an arbitrary rectangle can be computed using (11) and

$$\begin{aligned} \omega(x_1, x_2, y_1, y_2) &= \text{sgn}(x_2 y_2) \omega(|x_2|, |y_2|) - \\ &\quad \text{sgn}(x_2 y_1) \omega(|x_2|, |y_1|) - \\ &\quad \text{sgn}(x_1 y_2) \omega(|x_1|, |y_2|) + \\ &\quad \text{sgn}(x_1 y_1) \omega(|x_1|, |y_1|) \\ \text{sgn}(x) &= \begin{cases} 1 & \text{if } x \geq 0 \\ -1 & \text{if } x < 0. \end{cases} \end{aligned}$$

**Transmission Factors** A *transmission factor*,  $\tau$ , is the fraction of energy passing through a gas unimpeded. The transmittance of a gas depends on the absorption coefficient of the gas and the length of the path through the gas. A simple relationship for  $\tau$  can be determined by assuming that the absorptance of the gas (a local phenomena) is uniform throughout the gas layer. This factor, a decaying exponential, is given by

$$\tau(L) = e^{-aL}$$

where  $a$  is the absorptance of the gas per unit length and  $L$  is the path length. The gas absorptance is not calculated by the radiation exchange algorithms presented in this paper. Modak in [15] gives an algorithm for calculating gas absorptance from such information as soot concentration, partial pressures of CO, CO<sub>2</sub> *etc.* The emittance of the gas is the same as its absorption due to the gray gas assumption. The transmission factor,  $\tau$ , in the above equation is defined for one specific path through a gas. We are, however considering radiation exchange between a pair of finite area rectangles where many paths of different lengths occur. Siegel and Howell define an average transmission factor [7, p. 603] considering all possible paths between two surfaces through the gas. This form of  $\tau$  is defined to be

$$\overline{\tau}_{j-k} = \int \int_{A_j A_k} \frac{\tau(L) \cos(\theta_k) \cos(\theta_j)}{\pi L^2} dA_j dA_k / (A_j F_{j-k}).$$

For a hemisphere of radius  $L$ , this integral reduces to  $e^{-aL}$ . This integral can be estimated by finding a characteristic path with length  $\overline{L}$ , (a mean-beam length), such that

$$\overline{\tau}_{j-k} = e^{-a\overline{L}}.$$

For an optically thin gas, the mean beam length for radiation from an **entire** gas volume to the bounding surface (see [7]) is  $4V/A$  where  $V$  is the volume of the gas and  $A$  is the surface area of the region bounding the gas. This formula is not applicable in these calculations

since the radiation transfer of the gas to a wall surface is computed by splitting the **entire** gas volume into several pieces.

For the ten-wall model, the characteristic path is taken to be between the centers of two rectangles. This length is an underestimate of  $\overline{L}$ . This approximation breaks down when the two wall segments are close together or one of the wall segments is a complex shape (such as the union of four upper walls). The two and four-wall model estimates of  $\overline{L}$  are based upon an average distance between the rectangles that make up the wall segments.

For a given path between surface  $j$  and surface  $k$  we need to calculate the path length,  $L_U$ , through the upper layer and the path length,  $L_L$ , through the lower layer. Transmission factors for the upper and lower layers are then defined to be

$$\begin{aligned} \tau_{j-k}^U &= e^{-L_{j-k}^U a_U}, \\ \tau_{j-k}^L &= e^{-L_{j-k}^L a_L}. \end{aligned}$$

The energy fraction that passes through both layers is then

$$\tau_{j-k} = \tau_{j-k}^U \tau_{j-k}^L.$$

The energy fraction absorbed by a layer is just the fraction that doesn't pass through a layer or

$$\begin{aligned} \alpha_{j-k}^U &= 1 - \tau_{j-k}^U = 1 - e^{-L_{j-k}^U a_U}, \\ \alpha_{j-k}^L &= 1 - \tau_{j-k}^L = 1 - e^{-L_{j-k}^L a_L}. \end{aligned}$$

## Two, Four, Ten Wall Segment Radiation Exchange

Equation (1) for computing radiation exchange were specified in terms of general wall segments. This section discusses the radiation exchange computation in terms of a two-wall, four-wall and ten-wall model.

**Two-Wall Configuration Factors** The two-wall model combines the ceiling and four upper walls into one wall segment and the four lower walls and the floor into the second wall segment. The configuration factors for these two surfaces are derived by Quintiere in [16, Appendix] and are

$$\begin{aligned}
 F_{1-1} &= 1 - \frac{A_D}{A_1}, \\
 F_{1-2} &= \frac{A_D}{A_1}, \\
 F_{2-1} &= \frac{A_D}{A_2}, \\
 F_{2-2} &= 1 - \frac{A_D}{A_2}
 \end{aligned}$$

where  $A_1$ ,  $A_D$  and  $A_2$  are the areas of the extended ceiling, layer interface and extended floor respectively. These configuration factors are used in the original two-wall radiation model in BRI [3, 4] and in CFAST [5].

The two-wall model, RAD2, interacts with a four-wall heat conduction model in CFAST. The ceiling and upper wall temperatures may be different, so the question of how to represent the extended ceiling temperature arises. RAD2 chooses an extended ceiling temperature that results in the same energy contribution to the enclosure that a four-wall radiation algorithm would predict. The energy added to the room due to the ceiling and upper wall temperatures of  $T_{1a}$  and  $T_{1b}$  is

$$\sigma (A_{1a}\epsilon_{1a}T_{1a}^4 + A_{1b}\epsilon_{1b}T_{1b}^4).$$

where the subscripts  $1a$  and  $1b$  represents the ceiling and upper wall. We want to choose an effective or average temperature,  $T_{avg}$ , and emittance,  $\epsilon_{avg}$  for the extended ceiling that matches this energy contribution, or

$$\underbrace{\sigma (A_{1a} + A_{1b}) \epsilon_{avg} T_{avg}^4}_{\text{energy from extended ceiling}} = \underbrace{\sigma A_{1a} \epsilon_{1a} T_{1a}^4}_{\text{energy from ceiling}} + \underbrace{\sigma A_{1b} \epsilon_{1b} T_{1b}^4}_{\text{energy from upper wall}} \quad (12)$$

Choosing an average emittance computed using an average of  $\epsilon_{1a}$  and  $\epsilon_{1b}$  weighted by wall segment areas gives

$$\epsilon_{avg} = \beta \epsilon_{1a} + (1 - \beta) \epsilon_{1b}.$$

where  $\beta = A_{1a}/(A_{1a} + A_{1b})$ . Equation (12) can now be solved for  $T_{avg}$  using this value of  $\epsilon_{avg}$  to obtain

$$T_{avg} = \sqrt[4]{\gamma T_{1a}^4 + (1 - \gamma) T_{1b}^4}$$

where  $\gamma = A_{1a}\epsilon_{1a}/(A_{1a}\epsilon_{1a} + A_{1b}\epsilon_{1b})$ . A similar procedure could be used to compute an effective temperature and emittance for the extended floor.

**Four-Wall Configuration Factors** The configuration factors for four-wall radiation exchange are derived similarly to Quintiere's derivation for two walls in [16,

Appendix]. The setup for the following derivation is given in Figure 6. We wish to determine the configura-

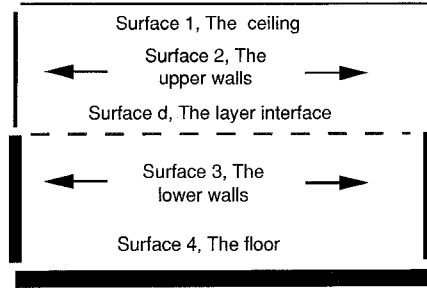


FIGURE 6: Schematic used to derive four wall configuration factor formulas.

tion factors

$$F_{i-j} \text{ for } i, j = 1, \dots, 4.$$

The 16 configuration factors can be determined in terms of  $F_{1-4}$ ,  $F_{1-d}$  and  $F_{4-d}$ .  $F_{1-4}$  does not change during a simulation since its value depends only on the height of the room and the area of the floor. Therefore,  $F_{1-4}$  only needs to be computed once. Configuration factors,  $F_{1-d}$  and  $F_{4-d}$  depend on the layer interface height so need to be calculated each time the radiation exchange is to be calculated. Configuration factors  $F_{1-4}$ ,  $F_{1-d}$  and  $F_{4-d}$  are determined using equation (10). Since  $A_1 = A_4$  it follows that  $F_{4-1} = F_{1-4}$ . The other 14 configuration factors can be calculated using simple algebraic formulas.

Since the floor and the ceiling is assumed to be a flat rectangular surface it follows that

$$F_{1-1} = F_{4-4} = 0.$$

Using the fact that configuration factors in an enclosure sum to 1 and that due to symmetry  $F_{2-1} = F_{2-d}$ , it follows that

$$F_{1-2} + F_{1-d} = 1, \quad (13)$$

$$F_{2-1} + F_{2-2} + F_{2-d} = 2F_{2-1} + F_{2-2} = 1 \quad (14)$$

Equations (13) and (14) can be solved for  $F_{1-2}$  and  $F_{2-2}$  respectively to obtain

$$F_{1-2} = 1 - F_{1-d}$$

$$F_{2-1} = \frac{A_1}{A_2} F_{1-2}$$

$$F_{2-2} = 1 - 2F_{2-1}$$

Similarly,

$$\begin{aligned} F_{4-3} &= 1 - F_{4-d} \\ F_{3-4} &= \frac{A_4}{A_3} F_{4-3} \\ F_{3-3} &= 1 - 2F_{3-4} \end{aligned}$$

Using the above configuration factors and equation (6) it follows that

$$\begin{aligned} F_{1-3} &= 1 - F_{1-4} - F_{1-2} \\ F_{3-1} &= \frac{A_1}{A_3} F_{1-3} \\ F_{3-2} &= 1 - F_{3-1} - F_{3-3} - F_{3-4} \\ F_{2-3} &= \frac{A_3}{A_2} F_{3-2} \\ F_{2-4} &= 1 - F_{2-1} - F_{2-2} - F_{2-3} \\ F_{4-2} &= \frac{A_2}{A_4} F_{2-4} \end{aligned}$$

**Ten-Wall Configuration Factors** To handle the more general radiation exchange case, a room is split into ten surfaces as illustrated in Figure 7. These surfaces are the

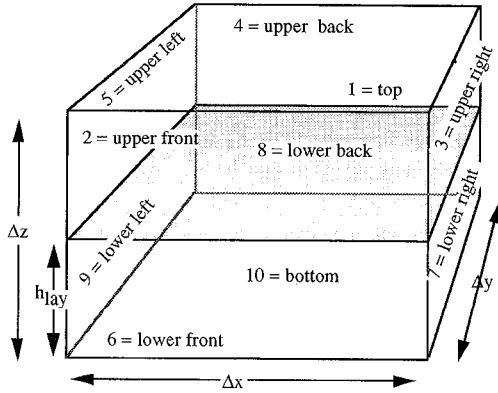


FIGURE 7: Schematic used for ten wall configuration factor formulas.

ceiling, four upper walls, four lower walls and the floor. The radiation exchange is computed between these ten surfaces and the intervening gas layer(s). In general, 100 configuration factors,  $F_{j-k}$  and 100 transmission factors  $\tau_{j-k}$  need to be determined each time this algorithm is invoked. Although there are 100 configuration factors for this room, only eight have to be calculated directly using equations (8) and (10). The other 92 can be com-

puted in terms of simple algebraic relationships using the properties outlined in equations (3) to (7). This reduction in required configuration factor calculations is due to the fact that the rectangle pairs 2 and 4, 3 and 5, 6 and 8 and 7 and 9 each have equal areas. The details of these calculations are documented in [14].

## SOLVING THE NET RADIATION EQUATIONS

### Solving The Net Radiation Equations Efficiently

The net radiation equation (1) is not diagonally dominant. Therefore, iterative methods should not be used to solve this equation unless it is suitably transformed. This can be done by substituting,  $\Delta q''_k = \epsilon_k \Delta \hat{q}''_k$  into equation (1) to obtain

$$\begin{aligned} \Delta \hat{q}''_k - \sum_{j=1}^N (1 - \epsilon_j) \Delta \hat{q}''_j F_{k-j} \tau_{j-k} &= \sigma T_k^4 - \\ &\sum_{j=1}^N \sigma T_j^4 F_{k-j} \tau_{j-k} - \frac{c_k}{A_k}. \end{aligned} \quad (15)$$

There are two reasons for solving equation (15) instead of (1). First, since  $\epsilon_k$  does not occur in the denominator, radiation exchange can be calculated when a wall segment emittance is zero. Second and more importantly, the matrix corresponding to the linear system of equations in (15) is diagonally dominant. When the number of wall segments is large and the wall segments have emittances close to one which often occurs in typical fire scenarios, the time required to solve this modified linear system can be significantly reduced due to this diagonal dominance by using iterative methods.

To see this, re-write equation (1) into matrix form to obtain

$$A \Delta q'' = B E - c \quad (16)$$

where the  $k, j$ 'th components of the  $N \times N$  matrices  $A$  and  $B$  are

$$a_{k,j} = \frac{\delta_{k,j}}{\epsilon_j} - F_{k-j} \tau_{j-k} \frac{1 - \epsilon_j}{\epsilon_j}, \quad (17)$$

$$b_{k,j} = \delta_{k,j} - F_{k-j} \tau_{j-k} \quad (18)$$

and the  $k$ 'th component of the vectors  $c''$  and  $E$  are

$$c_k'' = \frac{C_k}{A_k} = \sum_{j=1}^N (q_{j-k}''^{U,gas} + q_{j-k}''^{L,gas}) + \sum_{f=1}^{N_{fire}} q_{f-k}''^{fire}, \quad (19)$$

$$E_k = \sigma T_k^4, \quad (20)$$

and  $\delta_{k,j}$  is the Kronecker delta function,  $F_{k-j}$  is the configuration factor from the  $k$ 'th to the  $j$ 'th wall segment,  $\epsilon_j$  is the emittance of the  $j$ 'th wall segment,  $\tau_{j-k}$  is a fraction ranging from 0 to 1 indicating the amount of radiation that is transmitted through a gas. Also,  $q_{j-k}''^{U,gas}$  and  $q_{j-k}''^{L,gas}$  are radiation contributions due to the gas layers and  $q_{f-k}''^{fire}$  are radiation terms due to the  $f$ 'th fire. The matrix  $A$  can be transformed into a diagonally dominant matrix using the following scaling matrix,

$$D = \begin{pmatrix} \epsilon_1 & 0 & 0 \\ 0 & \ddots & 0 \\ 0 & 0 & \epsilon_N \end{pmatrix}$$

where  $\epsilon_k$  is the emittance of the  $k$ 'th wall segment. Define the scaled matrix  $\hat{A}$  by post-multiplying  $A$  by  $D$  and pre-multiplying  $\Delta q''$  by  $D^{-1}$  to obtain

$$\begin{aligned} \hat{A} &= AD \\ \Delta \hat{q}'' &= D^{-1} \Delta q'' \end{aligned}$$

Equation (16) then reduces to

$$\hat{A} \Delta \hat{q}'' = A \Delta q'' = BE - c.$$

Once the solution  $\Delta \hat{q}''$  is found we may recover the solution,  $\Delta q''$ , to the original problem by using  $\Delta q'' = D \Delta \hat{q}''$ .

The matrix  $\hat{A}$  is diagonally dominant which is now shown. Using the definition of  $a_{k,j}$  in equation (17) the  $kj$ 'th element of  $\hat{A}$  is

$$\hat{a}_{k,j} = a_{k,j} \epsilon_j = \delta_{k,j} - F_{k-j} \tau_{j-k} (1 - \epsilon_j). \quad (21)$$

A matrix is *diagonally dominant* if for each row the absolute value of the diagonal element is greater than the sum of the absolute values of the off diagonal elements or equivalently

$$|\hat{a}_{k,k}| > \sum_{\substack{j=1 \\ j \neq k}}^N |\hat{a}_{k,j}| \quad (22)$$

Substituting (21) into (22) we get the following requirement for  $\hat{A}$  to be diagonally dominant

$$1 - F_{k-k} (1 - \epsilon_k) \tau_{k-k} > \sum_{\substack{j=1 \\ j \neq k}}^N F_{k-j} (1 - \epsilon_j) \tau_{j-k}$$

or equivalently

$$1 > \sum_{j=1}^N F_{k-j} (1 - \epsilon_j) \tau_{j-k}.$$

The matrix  $\hat{A}$  is then diagonally dominant since  $1 > (1 - \epsilon_j) \tau_{j-k}$  and

$$1 = \sum_{j=1}^N F_{k-j} > \sum_{j=1}^N F_{k-j} (1 - \epsilon_j) \tau_{j-k}.$$

Iterative techniques for solving linear systems such as Gauss-Seidel are guaranteed to converge for diagonally dominant matrices [17, p. 542]. They also can be much more efficient than direct methods such as Gaussian elimination. The convergence speed depends on how small the right hand side of the above inequality is compared to 1. Physically, if the surfaces being modeled are approximate black bodies ( $\epsilon$  close 1) or the gas layers are thick ( $\tau$  close to 0) then iterative techniques for solving the net radiation equations will converge rapidly. Typical emittances for materials used in fire simulations range from  $\epsilon = .85$  to  $.95$ . For the limiting case when the wall materials are black bodies then the matrix  $\hat{A}$  is a diagonal matrix and iterative methods will converge in one iteration.

The advantage of using an iterative method over a direct method for computing radiation exchange between approximate black bodies increases as the number of wall segments increases. The cost of solving the linear system directly is proportional  $\frac{2}{3} N^3$  while the cost of using iterative techniques is proportional to  $kN^2$  where  $k$  is the number of iterations and  $N$  is the number of wall segments. Using Gauss-Seidel iterative methods, it has been found that convergence is achieved after two to three iterations for emittances around .9. The break-even point between iterative and direct methods for matrices of size 10 is about 6 or 7. The linear system for RAD2 and RAD4 is of size  $2 \times 2$  and  $4 \times 4$  respectively. Iterative methods are not faster for problems this small. RAD10 and problems with more wall segments can use iterative methods to decrease the time required to solve the linear system without sacrificing accuracy.

The radiation exchange equations can be solved analytically using Cramer's rule for the two wall segment case. This is how the radiation exchange equations were derived in [3] and [5]. Cramer's rule is not a good numerical technique to use for the solution of linear systems (even for  $2 \times 2$  systems) due to cancellation error that can be introduced when solving equations that are ill-conditioned.

### Algorithm for Calculating Four Wall Radiation Exchange

The strategy for computing the radiation exchange between four wall segments is outlined below. RAD4 performs these steps directly or calls subroutines that perform them. RAD2 and RAD10 follow the same logic.

#### Input

**Temperatures** Ceiling, Upper Wall, Lower Wall, Floor

**Emissivities** Ceiling, Wall, Floor

**Absorptivities** Upper, Lower Layer

**Fire** Size, Location, number

**Room** room number, dimensions, layer height

#### Output

**Flux** ceiling, upper wall, lower wall, floor

**Energy Absorption Rate** upper layer, lower layer

- Steps**
1. Calculate configuration factors, solid angles.
  2. Determine the effective length between each pair of wall segments. From these lengths and inputted layer absorptivities calculate transmission factors for surface  $j$  to surface  $k$
  3. Calculate transmission factors and gas layer absorptions for each fire  $f$  to surface  $k$ .
  4. Calculate the energy absorbed by each gas layer due to upper/lower gas layer emission and due to the fire(s) following Tables 2 and 3.
  5. Set up the linear algebra
    - (a) Define vector  $E$  using equation (20)
    - (b) Define matrix  $\hat{A}$  using equation (21)
    - (c) Define matrix  $B$  using equation (18)
    - (d) Define vector  $c$ , using equation (19) and Table 1.
  6. Solve the linear system

$$\hat{A}\Delta\hat{q}'' = BE - c \quad (23)$$

for  $\Delta q''$  net radiation leaving each surface where  $\Delta q''_k = \Delta\hat{q}''_k \epsilon_k$ . If the emissances are sufficiently close to 1 then use iteration to solve equation (23) otherwise use Gaussian elimination.

7. Calculate the energy absorbed by the upper and lower gas layers due to the total energy,  $q_k^{out}$  leaving each rectangle  $k$ .

## COMPUTATIONAL RESULTS

### Checks

Several simple checks can be made to verify a portion of the radiation calculation. First, no heat transfer occurs when all wall segments and both gas layers are at the same temperature. Therefore, the net radiation flux,  $\Delta q''_k$  given off by each surface and the energy absorbed by the gas should be zero under these uniform temperature conditions. Second, when there is no fire, the net energy absorbed by the gas must be the same as the net energy given off by the wall segments or equivalently

$q_{lower} + q_{upper} =$  energy absorbed by interior gases

$$\sum_{k=1}^N A_k \Delta q''_k$$

When the layers are transparent then the above equation sums to zero even though the individual wall fluxes  $\Delta q''_k$  will in general be non-zero. The gas absorbance terms,  $q_{lower}$  and  $q_{upper}$ , are computed by RAD2, RAD4 and RAD10. These values can be summed to verify that above equation is satisfied.

### Timings

Configuration calculations are one of the major bottlenecks in the radiation exchange calculation. Techniques to reduce the number of these calculations will improve the algorithms efficiency. A preliminary version of RAD4 was based on RAD10, a ten wall segment model. It computed 45 configuration factors directly. Subsequent versions of RAD4 computed eight and then two configuration factors directly. Table 4 summarizes the time required by these three different versions of RAD4. This table shows that the first version of RAD4 used approximately 70% of the time setting up the linear system and 30% solving it. Reducing the setup overhead by computing fewer configurations factors reduced

Table 4: Four Wall Radiation Algorithm Timings

Case	Total Time (s)	Linear Solve Time (s)
45 configuration factors and direct linear solve	0.2	0.06
Eight configuration factors and iterative linear solve	0.06	0.01
Two configuration factors and direct linear solve	0.012	0.001

the computation time required by a factor of 17. Why quibble over the timings of a subroutine that only took .2 seconds to execute to begin with? The relative impact of RAD4 on the zone fire model CFAST was measured by comparing the time required to execute DSOURC with and without RAD4. DSOURC is the subroutine CFAST uses to calculate the right hand side of the modeling differential equations. Most of the work is performed by this routine or routines that DSOURC calls. For a six room CFAST test case DSOURC took about .06 seconds. All times were measured on a Compaq 386/20 Deskpro. This computer has a 20mhz clock and uses a floating point accelerator (math co-processor). The actual times will be different on different computers. But the relative times and hence the conclusions should be the same. A routine that takes .2 seconds per room used in each room will result in a 21-fold increase in computer time since the ratio of the time in DSOURC with RAD4 to the time in DSOURC without RAD4 is  $(.2 * 6 + .06) / .06 \approx 21$ .

Even the fastest version of RAD4 will cause an increase of execution time of 2.25 if it is used in each room.

### Comparisons of RAD2 with RAD4

The predictions of a two wall radiation exchange model, RAD2, are compared with a four-wall model, RAD4. One of the assumptions made about N wall segment radiation models is that the temperature distribution of each wall segment is approximately uniform. The zone fire model CFAST models the temperature of four wall segments independently. Therefore, a two wall model for radiation exchange can break down when the temperatures of the ceiling and upper walls differ significantly. This could happen in CFAST, for example, when different wall materials are used to model the ceiling, walls and floor. To demonstrate this consider the following example.

To simplify the comparison between the two and

four wall segment models, assume that the wall segments are black bodies (the emissivities of all wall segments are one) and the gas layers are transparent (the gas absorptivities are zero). This is legitimate since for this example we are only interested in comparing how a two wall and a four wall radiation algorithm transfers heat to wall segments. Let the room dimensions be  $4 \times 4 \times 4$  [m], the temperature of the floor and the lower and upper walls be 300 [K]. Let the ceiling temperature vary from 300 [K] to 600 [K]. Figure 8 shows a plot of the heat flux striking the ceiling and upper wall as a function of the ceiling temperature. The two wall model predicts that the extended ceiling (a surface formed by combining the ceiling and upper wall into one wall segment) cools, while the four wall model predicts that the ceiling cools and the upper wall warms. The four-wall model moderates temperature differences that may exist between the ceiling and upper wall (or floor and lower wall) by allowing heat transfer to occur between the ceiling and upper wall. The two wall model is unable to predict heat transfer between the ceiling and the upper wall since it models them both as one wall segment.

A four-wall algorithm will also break down when the uniform temperature assumption is broken. This could occur when a fire is located nearer to one side of a room than another.

### CONCLUSIONS

This paper described algorithms for computing radiative heat exchange for three special cases, a two-wall, four-wall and ten-wall model. The theoretical basis for a general N wall model is well documented in the literature [7, 8, 9]. But an implementation of an N wall model is not yet practical for a zone fire model due to the high computational costs compared to other components in a zone fire model. One step was taken towards making N wall models practical. For wall surfaces that are approx-

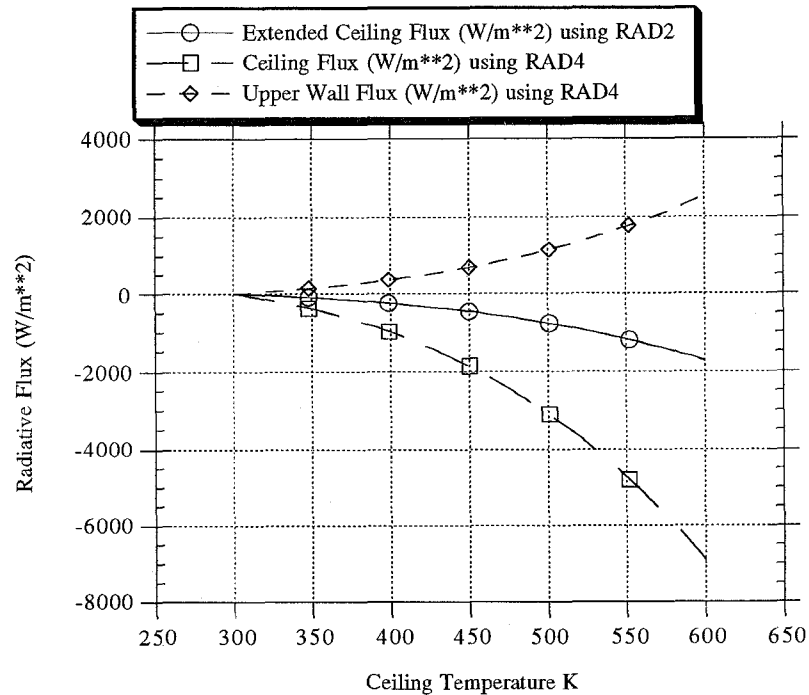


FIGURE 8: Comparison of wall surface fluxes computed using the two (RAD2) and four (RAD4) wall radiation model. The extended ceiling flux curve was computed using the two wall model (combining upper wall and ceiling). The ceiling and upper wall flux curves were computed using the four wall model.

imate black bodies ( $\epsilon > .85$ ) it was shown that the linear system of equations involving the unknown net radiative flux could be solved iteratively, reducing an  $o(N^3)$  to an  $o(N^2)$  problem. For specific cases, (four-wall, ten-wall) it was shown how to set up this linear system efficiently by avoiding unnecessary configuration factor calculations. For the general  $N$  wall problem it is not enough to solve the linear system efficiently. For example, in the ten-wall case the linear solve time is only 20% of the total solution time. Methods need to be found to calculate configuration factors more efficiently, perhaps at some cost in accuracy.

## NOMENCLATURE

$A$	area [ $m^2$ ]
$a$	absorption coefficient [ $m^{-1}$ ]
$A$	coefficient matrix for the net radiation equation.
$\hat{A}$	coefficient matrix for diagonally dominant version of the net radiation equation

$c$	vector of source terms used in the net radiation equation (1) to represent energy contributions to wall segments due to gas emitting layers and point source fires [W]
$B$	matrix used on the right hand side of the net radiation equation
$E$	emissive power, a vector whose $k$ 'th component is $\sigma T_k^4$
$D$	diagonal scaling matrix used to convert $A$ to the diagonally dominant version $\hat{A}$
$F_{j-k}$	geometric configuration factor, also called a view factor. The fraction of energy leaving a wall segment $j$ intercepted by wall segment $k$ .
$N$	number of wall segments
$N_{fire}$	number of fires
$q$	energy per unit time [W]
$\Delta q''$	net heat flux leaving a wall segment [ $W/m^2$ ]
$T$	temperature [K]
$\alpha$	absorbance

$\delta$	Kronecker delta function; $\delta_{ij} = \begin{cases} 0 & \text{if } i \neq j \\ 1 & \text{if } i = j \end{cases}$
$\epsilon$	emittance, fraction of the black body radiation emitted by a gray surface or gray gas.
$\chi$	fraction of a fire's energy release rate that contributes to radiative heat transfer.
$\phi$	configuration factor
$\pi$	universal constant
$\bar{\tau}$	average transmission factor where the average is computed over all possible paths between two wall segments
$\sigma$	Stefan-Boltzmann constant, $\sigma = 5.67 \times 10^{-8} \frac{\text{W}}{\text{m}^2\text{K}^4}$
$\tau$	transmittance, fraction of the energy passing through a gas unimpeded. If the gas has uniform absorbcency properties then $\tau$ can be computed using the Beer-Lambert law via $e^{-aL}$ where A is the absorbcency of the gas per unit length and L is the length of the path through the gas.
$\omega_{f-k}$	a solid angle; The energy fraction of the f'th fire striking the k'th wall segment.

### Subscripts

$j, k$	wall segments $j$ or $k$
$j - k$	from wall segment $j$ to wall segment $k$
$f$	fire $f$
$f - k$	from fire $f$ to wall segment $k$
$par$	parallel rectangles which are identical and opposite
$perp$	perpendicular rectangles which share a common edge
$total$	total energy release rate of a fire

### Superscripts

"	flux, a quantity per unit area
<i>fire</i>	a quantity due to a fire
<i>in</i>	incoming

<i>out</i>	outgoing
<i>L</i>	lower gas layer
<i>U</i>	upper gas layer
<i>L, gas</i>	a quantity due to the lower gas layer
<i>U, gas</i>	a quantity due to the upper gas layer
<i>i, gas</i>	a quantity due to the $i$ 'th gas layer where $i$ can be $L$ for lower or $U$ for upper layer

### REFERENCES

- [1] Henri E. Mitler and Howard W. Emmons. Documentation for cfc v, the fifth harvard computer fire code. NBS-GCR 344, National Institute of Standards and Technology, 1981.
- [2] Henri E. Mitler and John A. Rockett. User's guide to first, a comprehensive single-room fire model. Internal Report 3595, National Institute of Standards and Technology, 1987.
- [3] T. Tanaka. A model of multiroom fire spread. Internal Report 2718, National Bureau of Standards, 1983.
- [4] T. Tanaka. A model of multiroom fire spread. *Fire Science and Technology*, 3:105-121, 1983.
- [5] Walter W. Jones and Richard D. Peacock. Technical reference guide for FAST version 18. Technical Note 1262, National Institute of Standards and Technology, 1989.
- [6] Mark A. Dietenberger. Technical reference and user's guide for fast/ffm version 3. GCR 589, National Institute of Standards and Technology, 1991.
- [7] Robert Siegel and John R. Howell. *Thermal Radiation Heat Transfer*. Hemisphere Publishing Corporation, New York, second edition, 1981.
- [8] H. C. Hottel. *Heat Transmission*, chapter four. McGraw-Hill Book Company, New York, third edition, 1954.
- [9] H.C. Hottel and E.S. Cohen. Radiant heat exchange in a gas filled enclosure: Allowance for non-uniformity of gas temperature. *A I Ch E J*, 4, 1958.
- [10] Tokiyoshi Yamada and Leonard Y. Cooper. Algorithms for calculating radiative heat exchange between the surfaces of an enclosure, the smoke

layers and a fire, 1990. Un-published slides from a talk given as a Center for Fire Research Colloquium, July 20, 1990.

[11] Tokiyoshi Yamada. Algorithms for calculating radiative heat exchange between enclosure surfaces filled with smoke and a heat source, part i physical basis. Draft v.01, 1990.

[12] Richard D. Peacock, Glenn P. Forney, Paul Reneke, Rebecca Portier, and Walter W. Jones. CFAST, the Consolidated Model of Fire Growth and Smoke Transport. Technical Note 1299, National Institute of Standards and Technology, 1993.

[13] Frank P. Incropera and David P. De Witt. *Fundamentals of Heat and Mass Transfer*. John Wiley and Sons, New York, third edition, 1990.

[14] Glenn P. Forney. Computing radiative heat transfer occurring in a zone fire model. Internal Report 4709, National Institute of Standards and Technology, 1991.

[15] A. T. Modak. Radiation from products of combustion, FMRC No. OAOE6.BU-1. Technical report, Factory Mutual Corporation, 1978.

[16] J. Quintiere. A perspective on compartment fire growth. *Combustion Science and Technology*, 39:11-54, 1984.

[17] J. Stoer and R. Bulirsch. *Introduction to Numerical Analysis*. Springer-Verlag, New York, 1980.

5 riving at the  $k'$ th wall surface,  $q_j^{out} \tau_{j-k}^L \tau_{j-k}^U$  due to the  $j'$ th wall surface. . . . . 16

6 Configuration factor symmetries used to reduce number of direct configuration factor calculations. . . . . 17

7 Schematic used to derive four wall configuration factor formulas. . . . . 18

8 Schematic used for ten wall configuration factor formulas. . . . . 19

9 Comparison of wall surface fluxes computed using the two (RAD2) and four (RAD4) wall radiation model. The extended ceiling flux curve was computed using the two wall model (combining upper wall and ceiling). The ceiling and upper wall flux curves were computed using the four wall model. . . . . 20

**LIST OF TABLES**

1 Radiative Heat Flux Striking the  $k'$ th Rectangular Wall Segment . . . . . 21

2 Radiant Heat Absorbed by the Upper Layer 22

3 Radiant Heat Absorbed by the Lower Layer 23

4 Four Wall Radiation Algorithm Timings 24

**LIST OF FIGURES**

1 Input and Output Energy Distribution at the  $k'$ th Wall Surface . . . . . 13

2 Surface plot of temperature difference (original temperature and equivalent temperature accounting for vents and doors) as a function of fractional vent area and temperature showing the effect of vent openings on computing radiation heat transfer. . . . . 14

3 Schematic illustrating energy deposited into the lower layer,  $q_{f-k}^{fire} \alpha_{f-k}^L$ , deposited into the upper layer,  $q_{f-k}^{fire} \alpha_{f-k}^U \tau_{f-k}^L$ , and arriving at the  $k'$ th wall surface,  $q_{f-k}^{fire-L} \tau_{f-k}^U \tau_{f-k}^L$  due to the  $f'$ th fire. . . 15

4 Schematic illustrating energy deposited into the upper layer,  $q_j^{out} \alpha_{j-k}^U$ , deposited in lower layer,  $q_j^{out} \alpha_{j-k}^L \tau_{j-k}^U$ , and ar-

**LIST OF FIGURES**

1	Input and Output Energy Distribution at the k'th Wall Surface . . . . .	2
2	Surface plot of temperature difference as a function of fractional vent area and temperature showing the effect of vent openings on computing radiation heat transfer. . . . .	3
3	Schematic illustrating energy deposited into the lower layer, $q''_{f-k}^{fire} \alpha_{f-k}^L$ , deposited into the upper layer, $q''_{f-k}^{fire} \alpha_{f-k}^U \tau_{f-k}^L$ , and arriving at the k'th wall surface, $q''_{f-k}^{fire} \tau_{f-k}^L \tau_{f-k}^U$ due to the f'th fire. . . . .	4
4	Schematic illustrating energy deposited into the upper layer, $q''_j^{out} \alpha_{j-k}^U$ , deposited in lower layer, $q''_j^{out} \alpha_{j-k}^L \tau_{j-k}^U$ , and arriving at the k'th wall surface, $q''_j^{out} \tau_{j-k}^L \tau_{j-k}^U$ due to the j'th wall surface. . . . .	5
5	Configuration factor symmetries used to reduce number of direct configuration factor calculations. . . . .	6
6	Schematic used to derive four wall configuration factor formulas. . . . .	7
7	Schematic used for ten wall configuration factor formulas. . . . .	8
8	Comparison of wall surface fluxes computed using the two (RAD2) and four (RAD4) wall radiation model. The extended ceiling flux curve was computed using the two wall model (combining upper wall and ceiling). The ceiling and upper wall flux curves were computed using the four wall model. . . . .	9

**LIST OF TABLES**

1	Radiative Heat Flux Striking the k'th Rectangular Wall Segment . . . . .	10
2	Radiant Heat Absorbed by the Upper Layer . . . . .	11
3	Radiant Heat Absorbed by the Lower Layer . . . . .	12
4	Four Wall Radiation Algorithm Timings . . . . .	13